The oxidative degradation of dibenzoazepine derivatives by cerium(IV) complexes in acidic sulfate media

ARTICLE *in* DALTON TRANSACTIONS · NOVEMBER 2011

Impact Factor: 4.2 · DOI: 10.1039/c1dt11664a · Source: PubMed

4 AUTHORS:

Joanna Wiśniewska
Nicolaus Copernicus University
22 PUBLICATIONS **59** CITATIONS
SEE PROFILE

Grzegorz Wrzeszcz
Nicolaus Copernicus University
44 PUBLICATIONS **269** CITATIONS
SEE PROFILE

Marzanna Kurzawa
Nicolaus Copernicus University
35 PUBLICATIONS **134** CITATIONS
SEE PROFILE

Rudi van Eldik
Friedrich-Alexander-University of Erlangen-…
896 PUBLICATIONS **17,143** CITATIONS
SEE PROFILE

Dalton Transactions

Cite this: *Dalton Trans.*, 2012, **41**, 1259

www.rsc.org/dalton

PAPER

The oxidative degradation of dibenzoazepine derivatives by cerium(IV) complexes in acidic sulfate media†

Joanna Wiśniewska,*[a,b] Grzegorz Wrzeszcz,[a] Marzanna Kurzawa[a] and Rudi van Eldik[b]

Received 2nd September 2011, Accepted 18th October 2011
DOI: 10.1039/c1dt11664a

The kinetics of the oxidation of imipramine and desipramine using cerium(IV) complexes were studied in the presence of a large excess of azepine derivative (TCA) in acidic sulfate media using UV-Vis spectroscopy. The reaction proceeds *via* dibenzoazepine radical formation, identified by EPR measurements. The kinetics of the first degradation step were studied independently of the further slower degradation reactions. Linear dependences, with zero intercept, of the pseudo-first-order rate constants (k_{obs}) on [TCA] were established for both dibenzoazepine radical formation processes. Rates of reactions decreased with increasing concentration of the H^+ ion indicating that cerium(IV) as well as both reductants exist in an equilibrium with their protolytic forms. The activation parameters for the degradation of dibenzoazepine derivatives in the first oxidation stage were as follows: $\Delta H^{\neq} = 39 \pm 2$ kJ mol^{-1}, $\Delta S^{\neq} = -28 \pm 8$ J K^{-1} mol^{-1} for imipramine and $\Delta H^{\neq} = 39 \pm 2$ kJ mol^{-1}, $\Delta S^{\neq} = -28 \pm 6$ J K^{-1} mol^{-1} for desipramine, respectively. Imipramine and desipramine radicals dimerized leading to an intermediate radical dimer, which decayed in a first-order consecutive decay process. These two further reactions proceed with rates which are characterized by non-linear dependences of the pseudo-first-order rate constants (k_{obs}) on [TCA]. The degradation reaction of the intermediate radical dimer leads to an uncharged dimer as a final product. Mechanistic consequences of all the results are discussed.

Introduction

The role of cerium as the most effective oxidant and catalyst in many organic syntheses, is reflected in a number of reports in the literature.[1–11] Cerium chemistry is dominated by the +3 and +4 oxidation states. Among the lanthanides, cerium(IV) is characterized by the lowest standard redox potential $E^{\circ}(Ce^{IV}/Ce^{III}) = 1.70$ V.[12] Because of the high overpotential for water oxidation to oxygen the Ce^{IV} ion is stable in water and, though it is a strong oxidizing agent, has well-established aqueous chemistries. Cerium(IV) in redox processes reacts as an outer-sphere or inner-sphere mechanism in accordance with the type of the reductant.[13] Both $[Ce(H_2O)_9]^{3+}$ and $[Ce(H_2O)_7]^{4+}$ are very labile ions which exchange inner-sphere water molecules on a submicrosecond time scale.[14] In perchloric acid solutions with a non-coordinating anion, the redox potential for the Ce^{IV}/Ce^{III} couple increases from 1.70 to 1.78 V on increasing the $HClO_4$ concentration from 1 to 8 M, whereas in sulfuric acid solutions, it decreases from 1.44 to 1.42 V.[15] This trend is facilitated by the fact that the labile complex $[Ce(H_2O)_7]^{4+}$ undergoes a very fast complexation reaction with sulfate ions and forms a series of more stable cerium(IV) complexes: $[Ce(SO_4)_{aq}]^{2+}$, $[Ce(SO_4)_{2aq}]$, $[Ce(SO_4)_{3aq}]^{2-}$. Moreover, deprotonation of the aqua complex, which is a strong Brønsted acid leads to the hydroxo species: $[Ce(OH)_{aq}]^{3+}$, $[Ce(OH)_{2\,aq}]^{2+}$ and complicates the identity of the cerium(IV) in aqueous solutions.[16] Appropriate equilibrium constants (K_i) are presented in Table 1. Coordination of sulfate ions to cerium(IV) enables deprotonation of bisulfate because of the equilibrium between HSO_4^- and SO_4^{2-} ions in sulfuric acid solution and a certain percentage (ϕ_i), of aqua and sulfate cerium(IV) complexes results.

In this work cerium(IV) was used to oxidize imipramine (10,11-dihydro-*N*,*N*-dimethyl-5*H*-dibenz[*b*, *f*]azepine-5-propanamine) and desipramine (10,11 - dihydro - *N* - methyl-5*H* - dibenz [*b*,*f*]azepine-5-propanamine) (Scheme 1), which are well-known tricyclic antidepressants (TCA) and, in common with other substances from this group, are essential drugs, whose application is necessary in the therapy of many kinds of depression, including endogenic, organic and physicogenic ones.[17] Moreover, these drugs have also proved to be effective for the treatment of other illnesses in addition to depression.[18]

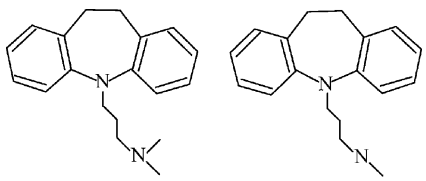

Imipramine Desipramine

Scheme 1

[a]*Department of Chemistry, Nicolaus Copernicus University, Gagarina 7, 87-100, Toruń, Poland*
[b]*Inorganic Chemistry, Department of Chemistry and Pharmacy, University of Erlangen-Nürnberg, Egerlandstr. 1, 91058, Erlangen, Germany*
† Electronic supplementary information (ESI) available. See DOI: 10.1039/c1dt11664a

Table 1 Acidity constants, formation constants (K_i) and percentage (ϕ_i) of sulfate cerium(IV) complexes[15]

$HSO_4^- \rightleftharpoons SO_4^{2-} + H^+$	$K_a = 10^{-1.99}$	$[Ce]\% = \frac{100}{1 + K_1[HL][H^+]^{-1} + K_1K_2[HL]^2[H^+]^{-2} + K_1K_2K_3[HL]^3[H^+]^{-3}}$
$Ce^{4+} + HSO_4^- \rightleftharpoons CeSO_4^{2+} + H^+$	$K_1 = 10^{3.5}$	$[CeSO_4^{2+}]\% = [Ce]\%K_1[HL][H^+]^{-1}$
$CeSO_4^{2+} + HSO_4^- \rightleftharpoons Ce(SO_4)_2 + H^+$	$K_2 = 10^{2.3}$	$[Ce(SO_4)_2]\% = [Ce]\%K_1K_2[HL]^2[H^+]^{-2}$
$Ce(SO_4)^2 + HSO_4^- \rightleftharpoons Ce(SO_4)_3^{2-} + H^+$	$K_3 = 10^{1.3}$	$[Ce(SO_4)_3^{2-}]\% = [Ce]\%K_1K_2K_3[HL]^3[H^+]^{-3}$
		$[Ce^{4+}]\% = \frac{[Ce]\%}{1 + K_{a1}[H^+]^{-1} + K_{a1}K_{a2}[H^+]^{-2}}$
$Ce^{4+} \rightleftharpoons Ce(OH)^{3+} + H^+$	$K_{a1} = 6.40$	$[Ce(OH)^{3+}]\% = [Ce^{4+}]\%K_{a1}[H^+]^{-1}$
$Ce(OH)^{3+} \rightleftharpoons Ce(OH)_2^{2+} + H^+$	$K_{a2} = 0.12$	$[Ce(OH)_2^{2+}]\% = [Ce^{4+}]\%K_{a1}K_{a2}[H^+]^{-2}$

One particularly important aspect of current research on the reactivity of dibenzoazephine derivatives is the nature of the degradation of these pharmaceutical preparations. This process is important, not only from the scientific, but also from practical point of view. The main aspect is the effective degradation and utilization of pharmaceutical preparations. Dibenzoazepines reveal a high resistance to redox transformation, however they may undergo partial degradation under the influence of reactive and effective oxidants such as cerium(IV). Only a few studies in the literature have discussed the oxidation reaction mechanism of the imipramine molecule,[19,20] which encouraged us to carry out a more complete study knowing the substantial importance of this kind of molecule in the medical and pharmaceutical fields. The purpose of this work is to gain an understanding the kinetics and mechanism of the oxidative degradation reaction of imipramine and desipramine by cerium(IV) in sulfuric acid solutions. According to Bishop *et al.*[21] dibenzoazepine derivatives are oxidized to a cation radical and subsequently converted into a dibenzoazepine dimer, which is oxidized to a dimeric dication. The overall oxidation process is four-electron. However, its mechanism has been proposed solely on the basis of voltammetry, cyclic voltammetry and amperostatic coulometry. As yet it has never been supported on the basis of kinetic and mechanistic studies.

Experimental

Materials

Imipramine hydrochloride (Sigma–Aldrich), desipramine hydrochloride (Sigma–Aldrich), $(NH_4)_4Ce(SO_4)_4{\cdot}2H_2O$ and all other chemicals were analytical grade reagents. Sulfuric acid solutions of the desired concentration were prepared from reagent grade H_2SO_4 (65%, Aldrich) and Na_2SO_4 was added in a few experiments to clarify the role of sulfates in the reactions of dibenzoazepine derivatives. For kinetic measurements, imipramine and desipramine hydrochlorides, and cerium(IV) salt were freshly prepared in H_2SO_4 solution just before mixing their solutions. Ultrapure water was obtained from a Milli-Q system (Millipore/Waters, Milford, MA, USA) and was used to prepare all the solutions.

EPR measurements

EPR spectra were recorded with a Radiopan EPR SE/X 2541 M spectrometer in X band (*ca.* 9.25 GHz) with a 100 kHz modulation. The microwave frequency was monitored with a frequency meter. The magnetic field was measured with an automatic NMR-type magnetometer. EPR spectra were recorded in room temperature using a both (i) stationary and (ii) continuous flow technique, and measurements were carried out from *ca.* 1 s after the initial mixing of the reagents. A flat quartz cell was used. The solution concentrations were [TCA] = (5–25) × 10^{-4} M, [Ce^{IV}] = (5–100) × 10^{-4} M, [H_2SO_4] = 1.0 M.

Stoichiometry

The stoichiometry of the overall reaction was studied using HPLC chromatography with UV-Vis detection on a Shimadzu HPLC chromatograph equipped with a C18 column (Supelco, 0.46 cm i.d., 15 cm i.l., 5 μm particles), a Rheodyne 7125 sample injector, a Shimadzu SPD-10A (VP) UV-Vis detector (250 nm) and a Shimadzu LC-10AD (VP) pump. A mobile phase composition (60 vol% of acetonitrile and 40 vol% of 20 mmol dm^{-3} Na_2HPO_4, pH = 7) was used for chromatographic separations.

An imipramine stock solution (1000 μg ml^{-1}) was prepared in a 100 ml volumetric flask by dissolving 0.1130 g imipramine·HCl in water. A cerium stock solution (0.3 mg ml^{-1} Ce) was prepared in a 100 ml volumetric flask by dissolving 0.144 g $(NH_4)_4Ce(SO_4)_4{\cdot}2H_2O$ in 0.1 M H_2SO_4. Working standard solutions were prepared by dilution of 0, 1, 2, 3, 4, 5 ml cerium stock solution (0, 3, 6, 9, 12, 15 μg ml^{-1}) in 100 ml volumetric flasks and 10 ml imipramine stock solution (100 μg ml^{-1}) in water. The HPLC measurements were performed in solutions of the drugs, which were used in excess over cerium(IV) concentrations analogous to the kinetic measurements. The degree of conversion in successive solutions was proportional to the decrease in the molarity of imipramine calculated from the area of its signal appearing after 13.5 min.

High-performance chromatography and mass spectra analysis of products

The chromatographic separations followed by a MS analyzer were run on a C18 column (Waters 100 mm × 2.1 mm i.d.). The injection volume was 20 μl and flow rate 0.6 ml min^{-1}. The composition of the gradient mobile phase (A: water containing 0.2% formic acid, B: acetonitrile containing 0.2% formic acid) was selected as follows: 0–1 min 2%B, 12 min 75%B, 18 min 90%B. Measurements were carried out on an HPLC system 1100 (Agilent Technologies, Waldbronn, Germany) equipped with a quaternary pump, UV-VIS detector, coupled with an Agilent 6410

Triple Quad LC/MS mass spectrometer equipped with an ESI interface and an ESI ion source. Mass spectra were collected under the following conditions: capillary temperature 300 °C, capillary voltage 4.5 kV, drying flow 9.0 l min^{-1} and nebulizer pressure 40 psi. The acquisition method used was previously optimized (capillary, magnetic lenses and collimating octapole voltages) in order to achieve maximum sensitivity. Mass spectra were collected in full scan positive mode in the range 100–850 mass-to-charge ratio (m/z).

Cyclic voltammetric measurements

Cyclic voltammetric (CV) measurements were performed in a one-compartment three-electrode cell with a gold working electrode (Metrohm) connected to a silver Ag/AgCl wire as pseudo-reference electrode and a platinum wire serving as counter electrode (Metrohm). Measurements were recorded with an Autolab PGSTAT 30 potentiostat at room temperature. The working electrode surface was cleaned using 0.05 mm alumina, and cleaned by ultrasonication followed by rinsing with high purity-water each time before use. The purpose of this pretreatment is to remove the organic impurities that may have remained or formed during the deposition of gold in the CVD chamber. The working volume of 10 ml (10 ml TCA, 10 ml cerium(IV), 5 ml TCA + 5 ml cerium(IV) added immediately before measurements) was deaerated by passing a stream of high-purity N_2 through the solution for 15 min prior to the measurements and then maintaining an inert atmosphere of N_2 over the solution during the measurements. All CVs were recorded for the reaction mixture with a sweep rate of 50 mV s^{-1}. The supporting electrolyte was 0.05 M H_2SO_4. The geometric area of the working electrode was estimated to be 0.7 cm^2.

Kinetic measurements

Spectra were recorded on a Hewlett-Packard 8453 "diode-array" spectrophotometer equipped with a thermostatted cell holder and Peltier Temperature Control System 89090A in a Tandem cuvette. Time-resolved spectra were recorded on an SX 18.MV Applied Photophysics apparatus, equipped with a J&M TIDAS diode-array detector. The stopped-flow measurements were carried out on a Carl Zeiss Jena VSU2-G equipped with a home-made stopped-flow accessory. In the experiments the concentration of cerium(IV) was fixed at 5×10^{-5} M. The concentration of dibenzoazepines used were in excess and were altered over the range $(0.5–5) \times 10^{-3}$ M for imipramine and $(0.5–3) \times 10^{-3}$ M for desipramine. The other experimental conditions were as follows: $[H_2SO_4] = 1.0$ M, $[H^+] = 1.2$ M, $I = 1.4$ M (H^+, HSO_4^-, SO_4^{2-}), $T = 283–298$ K. The rate was also analyzed at different H_2SO_4 concentrations: $[H_2SO_4] = 0.1–6.0$ M, $[H^+] = 0.1–7.2$ M, $I = 0.1–8.5$ M (H^+, HSO_4^-, SO_4^{2-}), $T = 283–298$ K. In a few cases, the rate was measured in 12 M H_2SO_4. The progress of the reaction was detected at 630 nm (λ_{max} for the azepine radical) and in some cases at 325 nm (electronic transitions in the cerium(IV) complexes region). Reactions were studied under pseudo-first-order conditions. Rate data were analyzed by a Gauss–Newton nonlinear least-squares fit to the first-order dependence of absorbance *vs.* time for the fast first oxidation process. Absorbance *vs.* time data were collected up to three half-lives ($3t_{1/2}$). The reported rate constants are the mean values of at least three determinations. The relative standard errors of the pseudo-first-order rate constants for a single kinetic trace were *ca.* 1–2% and relative standard errors of the mean value were usually *ca.* 1–2%. Two slower processes could not be separated and both rate constants were calculated from the two consecutive reaction scheme A → B → C and the non-linear least-squares fit to the two-exponential dependence of absorbance *vs.* time. The relative standard errors of the pseudo-first-order rate constants for a single kinetic trace were *ca.* 0.5–1%. The observed time scale for 95% reaction conversion for the oxidation process and the longer degradation reactions of the oxidation product for imipramine in 298 K were as follows: 0.03–0.3 s and 7.5–70 s, respectively. High pressure stopped-flow experiments were performed in the pressure range of 10 to 130 MPa on a custom built apparatus.[22] OLIS KINFIT software (Bogart, GA, 1989) was used for the analysis of kinetic traces. The pseudo-first-order rate constants were calculated from a one-exponential dependence of absorbance *vs.* time for the oxidation process and from a multi-exponential dependence for two consecutive longer degradation processes A → B → C. The reported rate constants are the mean values of at least four determinations.

Results and discussion

The reaction between dibenzoazepine hydrochloride derivatives (TCA) and cerium(IV) was followed in the aqueous acidic media ($[Ce^{IV}] = 5 \times 10^{-5}$ M, $[TCA] = (0.5–5) \times 10^{-3}$ M, $[H_2SO_4] = 0.1–6$ M, $[H^+] = 0.1–7.2$ M, $I = 0.1–8.5$ M (H^+, HSO_4^-, SO_4^{2-}), $T = 283–298$ K). The oxidation of chloride to chlorine by cerium(IV) in sulfuric acid solution does not occur at a measurable rate under ambient conditions, although this reaction is thermodynamically possible.[23,24] The progress of both the imipramine and desipramine reactions with cerium(IV) is reflected by marked changes in the electronic spectrum. The reason for these changes is the disappearance of the intensive yellow colored cerium(IV), which is reduced to a pale green cerium(III). Spectra presented in Fig. 1 reveal one absorption band of cerium(IV) at 330 nm with a molar absorption coefficient (5000–7000 M^{-1} cm^{-1}) depending on $[H_2SO_4]$.[25] Cerium(III) complexes, under conditions used in this work, are practically transparent in visible spectral region and exhibit only less intensive absorption bands at 295, 254, 241, 223, 212 nm (λ/nm (ε/M^{-1} cm^{-1}): 295 (40), 254 (1200), 241 (1100), 223 (700), 212 (600)).[26,27] The oxidation of dibenzoazepine derivatives leads to appearance of a dibenzoazepine radical (Scheme 2), which dimerizes and is oxidized to a blue-colored dimeric dication which absorbs intensively in the visible region (Fig. 1) at 609 nm (λ_{lit}/nm (ε_{lit}/M^{-1} cm^{-1}): 625 (29300)).[28]

As can be seen in Fig. 1, cerium(IV), which was used in sub-stoichiometric concentrations compared to the drug concentration, completely disappears in the time scale of appearance of the oxidation product of the dibenzoazepine, the blue-colored dimeric dication. Afterwards the dimer is decolorized in two consecutive processes, which proceed on a much longer time scale and are independent of the cerium(IV) concentration used in excess in other experiments. This former process is accompanied by a subsequent increase of absorbance in the electron-transition n–π^* band (λ_{max} 609 nm) appearing simultaneously with a decrease in the absorbance of the transition band at 325 nm assigned to cerium(IV) and by a sharp isosbestic point at 384 nm (Fig. 1A).

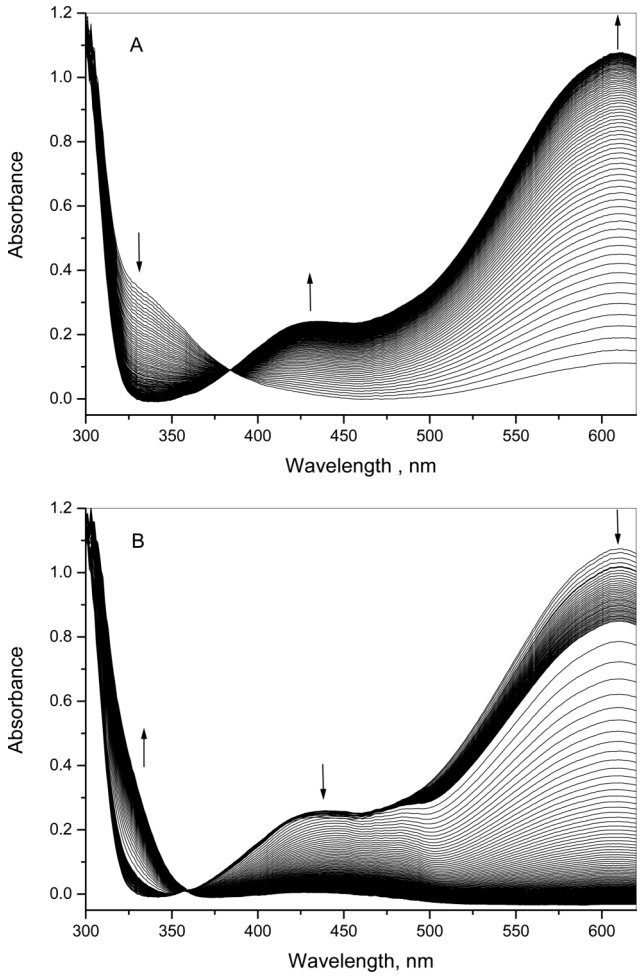

Fig. 1 Spectral changes observed during degradation of imipramine by cerium(IV). *Experimental conditions*: $[Ce^{IV}] = 1 \times 10^{-4}$ M, [TCA] = 1×10^{-3} M, $[H_2SO_4] = 0.5$ M, $[H^+] = 0.6$ M, $I = 0.685$ M (H^+, HSO_4^-, SO_4^{2-}), T = 5 °C, (A): $t = 1.5$ s, (B) $t = 1.5$–380 s.

Characteristic spectral changes for a second slow degradation of the dimeric dication are consistent with formation of a new band at 490 nm attributable to the next intermediate and of almost the same higher-energy band position at 440 nm and slow decrease of the absorbance in the electron-transition n–π^* band at 609 nm (Fig. 1B). A third slower process is consistent with the decrease of absorbance at 440 nm and significant blue shift of the higher-energy transition band from 440 to 430 nm, and slow decrease in the lower-energy electron-transition n–π^* band at 609 nm. These characteristic spectral changes are accompanied by sharp isosbestic points at 359 nm (Fig. 1B).

Formation of the $(TCA^{+\bullet})_2$ radical during oxidation of imipramine by the sulfato cerium(IV) complexes was observed using EPR spectroscopy. Fig. 2 shows the EPR spectrum of the reaction system after *ca.* 1.5 s from the initiation, and clearly indicates the presence of the radical. In the case of an equimolar ratio or excess of imipramine, the radical species is formed immediately and could be detected 1 s after mixing of the reaction solutions using a continuous flow technique. The initial EPR signal shows its maximum intensity and decayed after *ca.* 10–100 s. The intensity changes of the signal correlate with the decay time of the $(TCA^{+\bullet})_2$ radical. Nevertheless, these experiments were performed

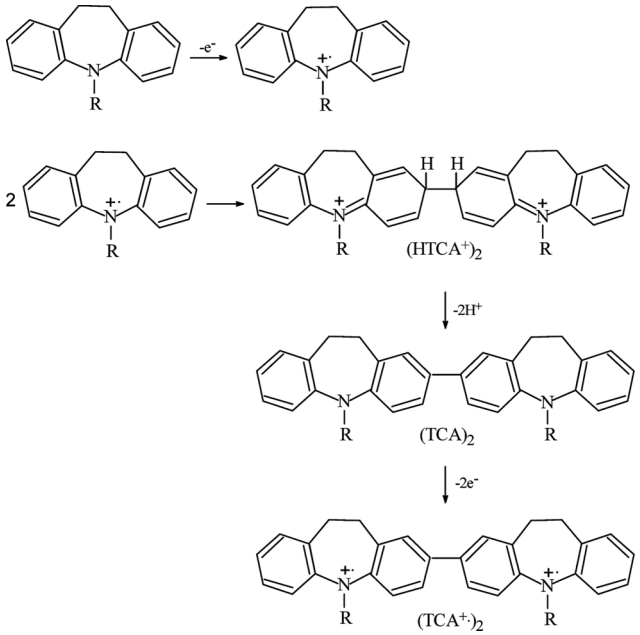

Scheme 2

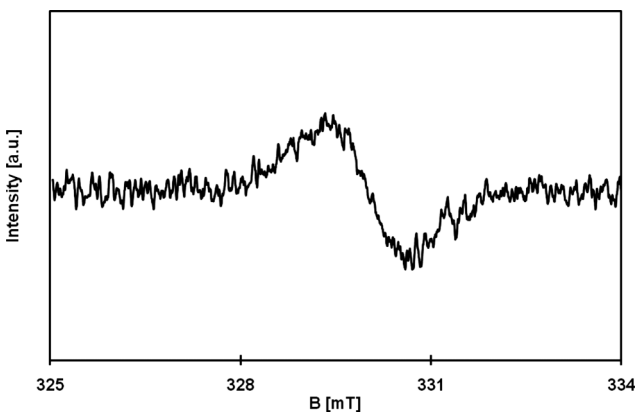

Fig. 2 EPR spectrum recorded for 3.65×10^{-3} M imipramine and 1.35×10^{-3} M cerium(IV) in 1 M H_2SO_4. Other conditions: continuous flow technique, time of reaction, *ca.* 1.5 s, microwave frequency 9.24886 GHz, room temperature.

at different temperatures (EPR at room temp., spectral analysis at 5° C). The EPR spectra of the $(TCA^{+\bullet})_2$ radicals exhibit a single nearly isotropic line with $g = 2.0022 \pm 0.0008$ and peak-to-peak width, $\Delta B_{pp} \sim 1.2$ mT. The spectrum remains poorly resolved due to the large number of lines, the relatively low spin density of the unpaired electron at the lateral ring protons, and also incomplete averaging of the g factor and/or hyperfine anisotropy. It was also observed that the initial intensity of the EPR signal was not so high and quickly decreased during the course of reaction. Finally, the EPR signal disappeared by further radical oxidation or degradation. A two-fold excess of Ce(IV) using a continuous flow technique (1–5 s) gives radical species but using a stationary technique their intensity increased to the highest value after *ca.* 25 s and then decayed. A four-fold excess of Ce(IV) using a continuous flow technique (1–5 s) gives no radical species but under stationary technique another radical slowly forms. In this case, the intensities of the radical EPR signal increase, reach a maximum after *ca.*

50 s and then decay. The intensity changes of the signal at g = 2.0022 do not correlate with the absorbance changes at λ_{max} = 609 nm discussed above for higher molar ratios of cerium(IV). The EPR parameters are the same as above (within experimental error). In the case of the two-fold excess of Ce(IV), the signal has the highest value of intensity as compared with other Ce(IV) to imipramine ratios (if all other experimental parameters are kept constant), which is in agreement with a molar ratio TCA : Ce(IV) of 1 : 2 (Scheme 2). The stoichiometry for the overall process was determined experimentally using HPLC analysis in an excess of TCA and was equal to 1 : 1.5.

The kinetics of the overall process were studied in 1 M H_2SO_4 in two separate series of experiments corresponding to the oxidation of dibenzoazepines by cerium(IV) and degradation reactions of their oxidation products due to a large difference in the rate between the first and the further second and third processes. In the preliminary experiments, the kinetic traces were scanned independently at 325 nm (in the cerium(IV) band) and at 609 nm (in the dibenzoazepines oxidation product band) for the fast oxidation process. Cerium(IV) disappeared on the same time scale as the $(TCA^{+\bullet})_2$ was forming. The pseudo-first-order rate constants calculated for kinetic traces at 325 and 609 nm do not differ in sulfuric acid solution in the range of statistical error (greater at 325 nm). In stopped-flow measurements the first few percent of reaction could not be detected and have been omitted because of mixing-time of the stopped-flow spectrophotometer. For the second and third slower degradation reactions proceeding *via* two consecutive processes, kinetic traces were collected at 630 nm and obey satisfactory a two-exponent dependence of absorbance *vs.* time.[29]

An effect of [TCA] on the oxidative degradation reaction course was studied by varying its initial concentration used in excess. The observed rate constants (Table S1, ESI†) revealed linear dependences *vs.* [TCA] with zero intercepts as expected for the irreversible reaction dibenzoazepines with cerium(IV) (Fig. 3). The rate law characterizing this concentration dependence can be expressed by the equations:

$$-\frac{d[TCA]}{dt} = -\frac{d[Ce^{IV}]}{dt} = k_1[Ce^{IV}][TCA] \quad (1)$$

where the second-order rate constant for the forward reaction, k_1, according to eqn (1), was obtained from the slope (Fig. 3). The linear regression data for this reaction are presented in Table 2. The observed rate constant slowly decreased with increasing concentration of H_2SO_4 (Fig. 4) and decrease with increasing concentration of sulfate even when the acidity decreased simultaneously as a consequence of an increase of the concentration of Na_2SO_4 (0.25 M–1.0 M) added to the 1.0 M H_2SO_4 solution (Fig, S1, ESI†).

The observed rate constants for the second (Fig. 5) and third slower process (Fig. 6) revealed quadratic dependences *vs.* [TCA] with no significant intercepts in the case of this last process. These data were fitted by a parabolic dependence, in which the k_2 and k_3 terms represent the third-order rate constants for the forward reactions, according to the equations:

$$-\frac{d[(TCA^{+\bullet})_2]}{dt} = (k_{-2} + k_2[TCA]^2)[(TCA^{+\bullet})_2] \quad (2)$$

Table 2 Linear regression data for k_{obs} *vs.* [TCA] for the electron-transfer reaction between cerium(IV) complexes and imipramine or desipramine. *Experimental conditions*: $[Ce^{IV}] = 5 \times 10^{-5}$ M, [TCA] = (0.5–3) × 10^{-3} M, $[H_2SO_4]$ = 1.0 M, $[H^+]$ = 1.2 M, I = 1.4 M (H^+, HSO_4^-, SO_4^{2-})

TCA	T/K	$10^{-3}k_1/M^{-1}$ s^{-1} Slope	k_{-1}/s^{-1} Intercept
Imipramine	283	10.5 ± 0.3	2.0 ± 1.3
	288	14.0 ± 0.7	3.2 ± 1.4
	293	20.1 ± 0.8	1.8 ± 1.2
	298	23.9 ± 1.2	1.5 ± 1.6
Desipramine	283	13.0 ± 0.3	2.5 ± 0.5
	288	17.4 ± 0.5	3.2 ± 1.0
	293	24.5 ± 1.2	−1.3 ± 2.3
	298	29.3 ± 1.1	0.7 ± 1.9

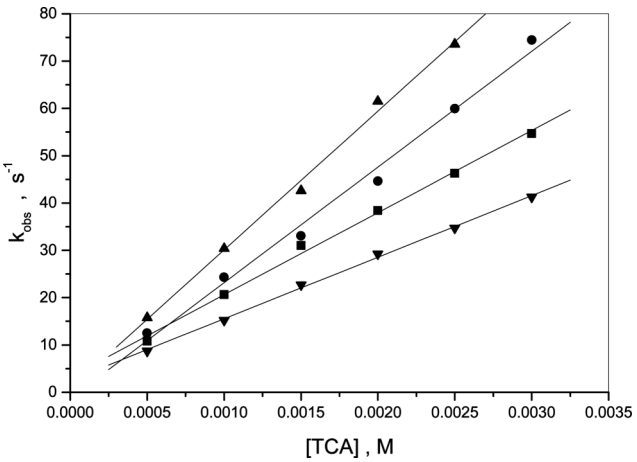

Fig. 3 Plots of k_{obs} *vs.* [TCA] for the electron-transfer reaction between desipramine and cerium(IV) at different temperatures. *Experimental conditions*: $[Ce^{IV}] = 5 \times 10^{-5}$ M, $[H_2SO_4]$ = 1.0 M, $[H^+]$ = 1.2 M, I = 1.4 M (H^+, HSO_4^-, SO_4^{2-}), T = 283 (▼), 288 (■), 293 (●), 298 (▲) K.

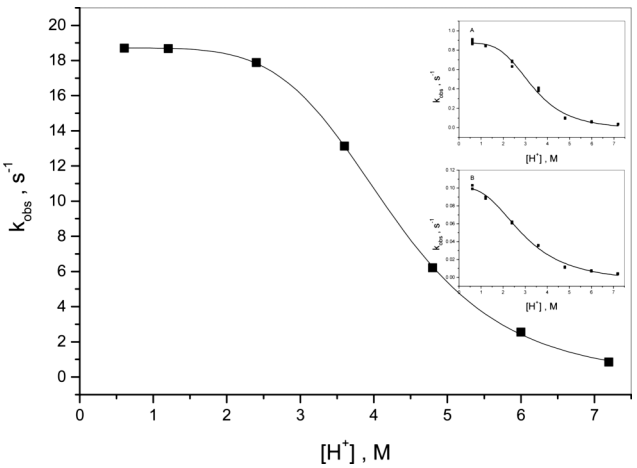

Fig. 4 Plot of k_{obs} *vs.* $[H^+]$ for the electron-transfer reaction between imipramine and cerium(IV). Inset: (A): the second reaction step, (B): the third reaction step. *Experimental conditions*: $[Ce^{IV}] = 5 \times 10^{-5}$ M, [IMI] = 1×10^{-3} M, $[H_2SO_4]$ = 1.0 M, $[H^+]$ = 1.2 M, $I \neq$ const, T = 288 K.

$$-\frac{d[(HTCA^{+})_2]}{dt} = (k_{-3} + k_3[TCA]^2)[(HTCA^{+})_2] \quad (3)$$

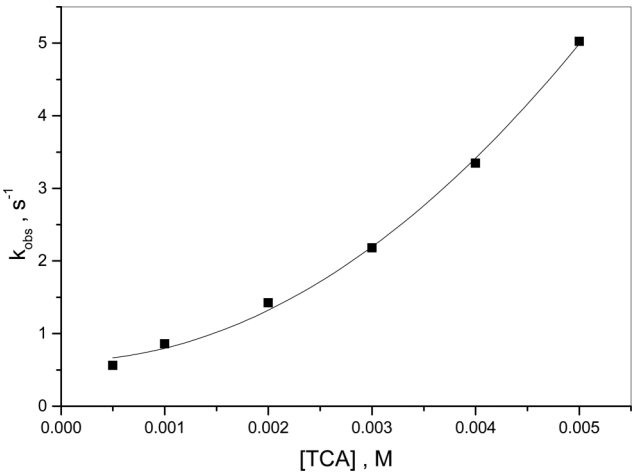

Fig. 5 Plot of k_{obs} *vs.* [TCA] for the second degradation step of imipramine. *Experimental conditions*: $[Ce^{IV}] = 5 \times 10^{-5}$ M, $[H_2SO_4] = 1.0$ M, $[H^+] = 1.2$ M, $I = 1.4$ M (H^+, HSO_4^-, SO_4^{2-}), $T = 288$ K.

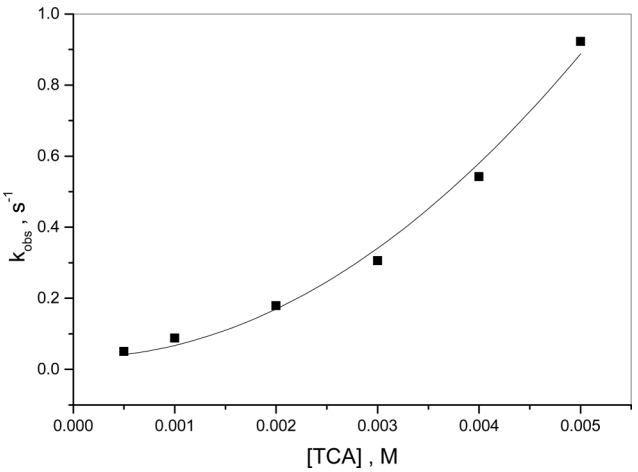

Fig. 6 Plot of k_{obs} *vs.* [TCA] for the third degradation step of imipramine. *Experimental conditions*: $[Ce^{IV}] = 5 \times 10^{-5}$ M, $[H_2SO_4] = 1.0$ M, $[H^+] = 1.2$ M, $I = 1.4$ M (H^+, HSO_4^-, SO_4^{2-}), $T = 288$ K.

The k_{-3} term was close to zero and was omitted in the further discussion. All the regression data are presented in Tables 3 and 4. The observed rate constant decreased slightly with increasing concentration of H_2SO_4 and revealed the sigmoid dependences similar to that for first step over the same pH range (Fig. 4) and is almost unaffected by the concentration of sulfate despite the decrease in acidity after addition of Na_2SO_4 (0.25 M–1.0 M) to the 1.0 M H_2SO_4 solution and an increasing ionic strength (Figure S1, ESI†).

The reaction with cerium(IV) proceeds according to an outer-sphere mechanism. This conclusion may be supported by the fact that the second-order rate constant for 1.0 M H_2SO_4 was very similar to the value for 1.0 M $HClO_4$ even though the percentage fraction of $[Ce(OH)]^{3+}$ ion is equal to 86% whereas in sulfuric acid it is reduced to 2.5×10^{-5}%. From the other point of view the redox potential of Ce^{IV}/Ce^{III} couple does not change in 0.1–6 M sulfuric acid. This is because the value of $[HSO_4]^n[H^+]^{-n}$ is constant and the ratio of $[Ce(SO_4)_{aq}]^{2+}$, $[Ce(SO_4)_{2aq}]$, $[Ce(SO_4)_{3aq}]^{2-}$ and aqua complexes are stable as long as sulfate salts are not added to the sulfuric acid solution. Only in the mixture of

Table 3 Parabolic regression data for k_{obs} *vs.* [TCA] for the second step of the degradation reaction of azepine dimer. *Experimental conditions*: $[Ce^{IV}] = 5 \times 10^{-5}$ M, [TCA] = (0.5–5) × 10^{-3} M, $[H_2SO_4] = 1.0$ M, $[H^+] = 1.2$ M, $I = 1.4$ M (H^+, HSO_4^-, SO_4^{2-})

TCA	T/K	$10^{-4}k_2$/M^{-2} s^{-1}	k_{-2}/s^{-1}
Imipramine	283	13.1 ± 0.2	0.41 ± 0.02
	288	17.4 ± 0.4	0.60 ± 0.05
	293	24.2 ± 1.1	1.19 ± 0.14
	298	40.5 ± 1.3	1.10 ± 0.16
Desipramine	283	16.9 ± 0.3	0.31 ± 0.01
	288	21.8 ± 0.6	0.38 ± 0.03
	293	31.8 ± 0.8	0.60 ± 0.05
	298	37.6 ± 1.0	0.80 ± 0.05

Table 4 Parabolic regression data for k_{obs} *vs.* [TCA] for the third step of the degradation reaction of azepine dimer. *Experimental conditions*: $[Ce^{IV}] = 5 \times 10^{-5}$ M, [TCA] = (0.5–5) × 10^{-3} M, $[H_2SO_4] = 1.0$ M, $[H^+] = 1.2$ M, $I = 1.4$ M (H^+, HSO_4^-, SO_4^{2-})

TCA	T/K	$10^{-3}k_3$/M^{-2} s^{-1}	k_{-3}/s^{-1}
Imipramine	283	24.5 ± 0.4	0.03 ± 0.01
	288	34.3 ± 0.9	0.03 ± 0.01
	293	47.9 ± 1.0	0.08 ± 0.01
	298	65.0 ± 1.3	0.04 ± 0.02
Desipramine	283	24.0 ± 0.4	0.02 ± 0.01
	288	32.0 ± 0.7	0.03 ± 0.01
	293	46.1 ± 0.7	0.05 ± 0.01
	298	57.5 ± 0.7	0.08 ± 0.01

sulfuric or different acid and sulfate salts, the percentages of the various species might be changed on changing the concentration of sulfate ions. With increasing H^+ concentration, the fraction of $[Ce(OH)_{aq}]^{3+}$ decreases but it is not certain that a substantial decrease in the rate of the relevant reaction in increasing H^+ concentration is accompanied by the same trend of change of the $[Ce(OH)_{aq}]^{3+}$ concentration because the total concentration of aqua cerium(IV) complexes is very low in sulfuric acid solutions. As mentioned above, because the relative proportions of various complexes calculated for different $[H_2SO_4]$ are stable over a wide range of the H^+ concentrations, cerium(IV) exists in sulfate acidic media mostly (92%) as $[Ce(SO_4)_{3aq}]^{2-}$ and this species seems to be an effective oxidant in the reaction with dibenzoazepines.

The k_{obs} dependence on $[H^+]$ for oxidation and further degradation processes can reflect greater reactivity of the conjugate base of the reductant, whose concentration decreases with increasing H^+ concentration. The protonation effect observed in the most concentrated sulfuric acid solution suppressed the oxidative degradation reaction of these substances and the further slower degradation steps. This means that not only the dibenzoazepine derivatives but also the dimers exist in their protolytic form. This fact can be proved by the bathochromic shift of the dimer electron-transition spectral band from 609 nm in 1 M H_2SO_4 to 630 nm in 12 M H_2SO_4. This change of spectral band position in the absorption spectrum might arise from protonation of the nitrogen atom in the heterocyclic azepine ring.

In the proposed reaction scheme (Scheme 2), the oxidation of dibenzoazepine derivatives to the radical is the rate-determining step. The proton-release step probably does not occur effectively and the intermediate $(HTCA^+)_2$ dimer is immediately oxidized

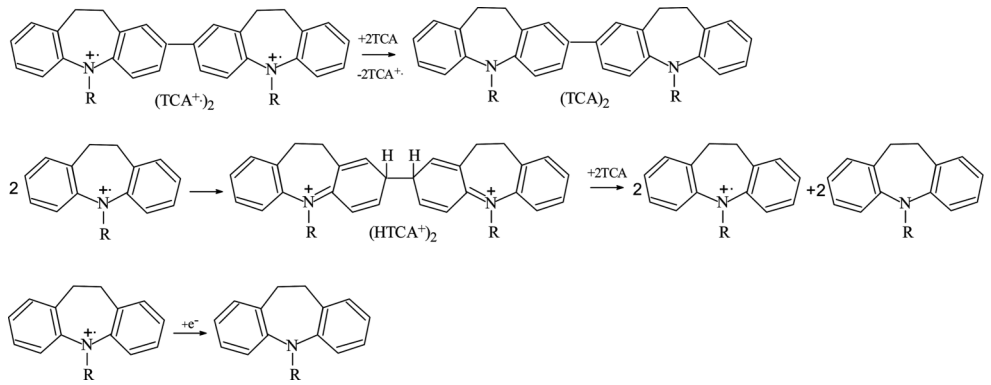

Scheme 3

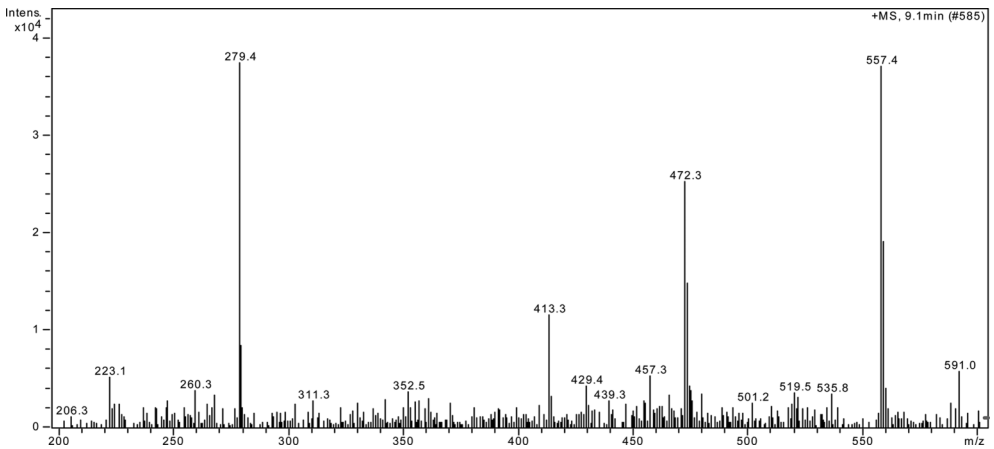

Fig. 7 ESI-MS spectra of the $(TCA)_2$ dimer. *Experimental conditions* for HPLC: gradient mobile phase composition (A: water containing 0.2% formic acid, B: acetonitrile containing 0.2% formic acid), C18 column (Waters 100 mm × 2.1 mm), injection volume 20 µl, flow rate 0.6 ml min^{-1}.

in the next fast process to the radical $(TCA^{+\bullet})_2$ dication; only this process is connected with two proton release. In 1 M H_2SO_4, the intermediate $(HTCA^+)_2$ appears only in the next slower comproportionation reaction of $(TCA^{+\bullet})_2$ with TCA. In concentrated 70% sulfuric acid solution, the $(HTCA^+)_2$ dimer is a final product and is not oxidized to the radical $(TCA^{+\bullet})_2$ dication. The high concentration of H^+ suppresses proton release and the further oxidation process does not occur. In this medium, the blue $(HTCA^+)_2$ dimer is stable for weeks and does not undergo further degradation processes. No EPR signal was detected in the concentrated 70% sulfuric acid solution suggesting that the $(HTCA^+)_2$ dimer has no radical character. Further slower processes of the intermediate $(TCA^{+\bullet})_2$ radical degradation are presented in Scheme 3. In the first reaction of $(TCA^{+\bullet})_2$ with TCA the final product $(TCA)_2$ and $TCA^{+\bullet}$ radical are produced. The $TCA^{+\bullet}$ radical dimerizes as before and the next $(HTCA^+)_2$ intermediate appears, which is unstable in 1 M H_2SO_4 and in excess of TCA reacts with reducing agent.

The final product $(TCA)_2$ was detected by HPLC-ESI-MS. The chromatogram revealed only the presence of two fractions characteristic of imipramine with a retention time of 9.5 min and dimer $(TCA)_2$ with retention time shorter than for imipramine of 9.1 min and low relative abundance. Electron spray ionization MS spectra (Fig. 7) show the presence of characteristic fragmentation peaks for the dimer: 557 (M – H), 472 (M – $C_5H_{12}N$), 279 (M – $C_{19}H_{22}N_2$ monomer) *m*/*z*. We conclude on the basis of analysis of their fragmentation peaks, that the product mass should be 558. The molecular and fragmentation peaks for imipramine were as follows: 281 (MH^+), 236 (M – C_2H_6N), 208 (M – $C_4H_{10}N$), 86 (M – $C_4H_{12}N$) *m*/*z*.

CV measurements of cerium(IV) solution in the presence of imipramine were performed in order to determine the interaction between these two species in the reaction mixture. Only a few studies in the literature have mentioned the oxidation reaction mechanism of the imipramine molecule.[21,30,31] The electrochemistry and cyclic voltammetry of imipramine have been studied intensively by Bishop[21] at a gold electrode in 0.1 M H_2SO_4. These CV measurements revealed the electrochemical oxidation of imipramine to a radical and further oxidation of dimer appearing after dimerization of the radical. The dimer is more easily oxidized than the monomer and two next amalgamated peaks appeared at slightly lower potentials than that for monomer. Ivandini *et al.*[30] reported a cyclic voltammetric study of imipramine at a boron-doped diamond electrode and glassy carbon electrode. These authors concluded that electrochemical oxidation of imipramine occurs *via* a two-electron one-proton mechanism in analogy to that for methyliminobibenzyl.[19,32] Our CV measurements were performed at a potential sweep rate of 50 mV s^{-1} in 0.05 M H_2SO_4 at a gold electrode. The cyclic voltammogram of 5×10^{-3} M imipramine revealed one quasi-reversible oxidation peak at 1.12 V *vs.* Ag/AgCl and two amalgamated peaks at 0.93 and 0.75 V, which disappeared after the first few cycles (Fig. 8A). These two

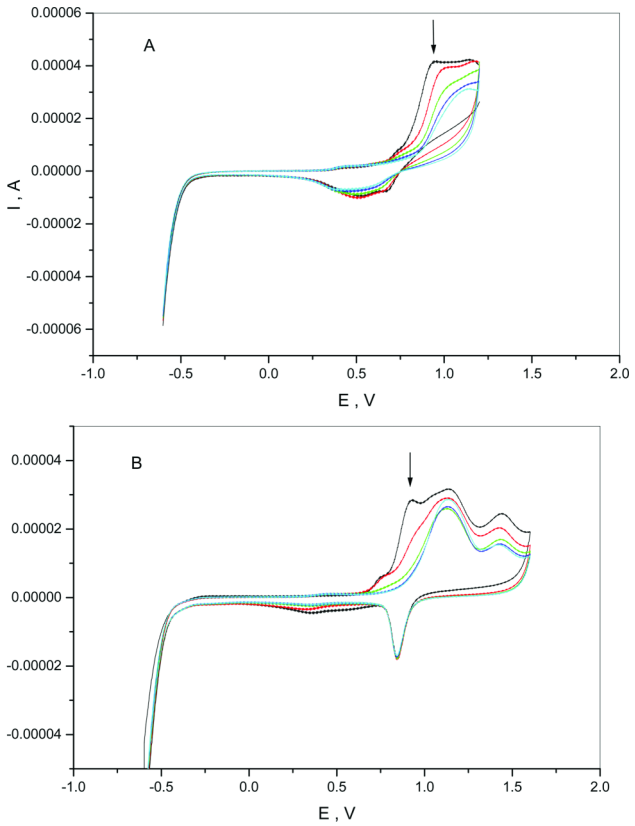

Fig. 8 CV of imipramine and the reaction mixture of imipramine and cerium(IV). *Experimental conditions*: (A): [TCA] = 5×10^{-3} M, [H_2SO_4] = 0.05 M; (B): [TCA] = 5×10^{-3} M, [Ce^{IV}] = 5×10^{-3} M, [H_2SO_4] = 0.05 M, scan rate = 0.05 V s^{-1}, 5 scans, T = 295 K.

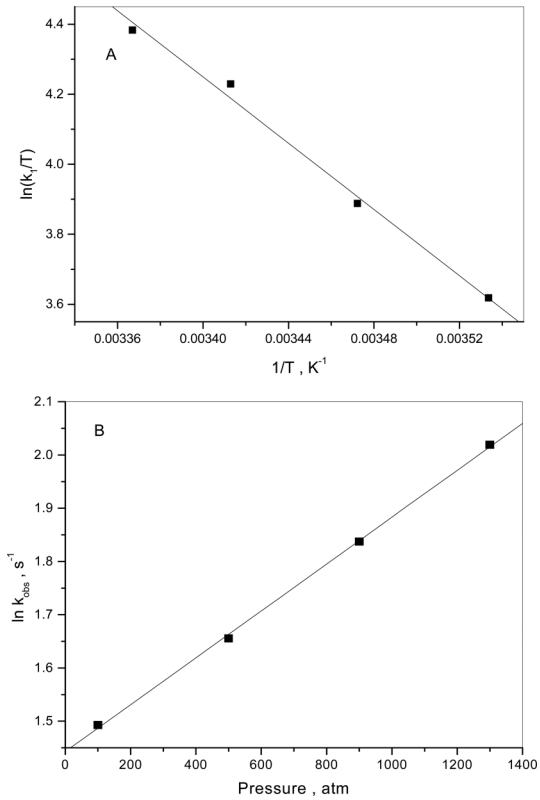

Fig. 9 (A): Eyring plot of $\ln(k_1/T)$ *vs.* $1/T$ for the electron-transfer reaction between imipramine and cerium(IV). *Experimental conditions*: [Ce^{IV}] = 5×10^{-5} M, [TCA] = $(0.5–5) \times 10^{-3}$ M, [H_2SO_4] = 1.0 M, [H^+] = 1.2 M, I = 1.4 M (H^+, HSO_4^-, SO_4^{2-}), T = 283–298 K, λ = 630 nm. (B): plot of $\ln(k_1)$ *vs.* pressure. *Experimental conditions*: [Ce^{IV}] = 5×10^{-5} M, [TCA] = 5×10^{-4} M, [H_2SO_4] = 1.0 M, [H^+] = 1.2 M, T = 278 K, λ = 630 nm.

last peaks are accompanied by oxidation of the dimer. In 5×10^{-3} M cerium(IV) in the absence of imipramine one reversible oxidation peak at 1.33 V is observed in the CV voltammogram (*vs.* Ag/AgCl) and one reduction peak at 0.85 V, corresponding to the one-electron Ce^{IV}/Ce^{III} couple. In the 5×10^{-3} M cerium(IV) and 5×10^{-3} M imipramine mixture, all peaks mentioned above appeared in the CV voltammogram and the reversible oxidation peak characteristic of cerium(IV) is only slightly shifted to the higher potential with reference to the cerium(IV) solution and successively decreases, as peaks corresponding to oxidation of the dimer increase during the first five scans (Fig. 8B).

The activation parameters for the electron transfer reaction and the next two degradation processes are presented in Table 5. The enthalpy and entropy of activation were calculated from an Eyring plot of $\ln(k/T)$ *vs.* $1/T$, where k is the second-order (k_1) or third-order rate constants (k_2 and k_3) for the fast and both slower degradation processes, respectively (Fig. 9A and S2, ESI†). An effect of pressure on the kinetics of these reactions was studied over the pressure range 10–130 MPa. Plots of $\ln(k_{obs})$ *vs.* pressure were found to be linear and enabled to determine the volume of activation ($\Delta V^{\neq}$) (Fig. 9B and S3–S4 , ESI†). As was mentioned above, the k_{-3} term was close to zero and the contribution of k_{-2} to $k_{obs\,(2)}$ can be neglected and $k_{obs\,(2)} = k_2[TCA]^2$. For that reason, the $\Delta V^{\neq}$ could be calculated also for these two slow processes. Pressure experiments were repeated at least two times, and the reported $\Delta V^{\neq}$ values were calculated as the mean value. The high-pressure kinetic data are presented in Table S2 (see ESI†). As can be seen, all reaction steps proceed with a negative entropy of activation and exhibit a negative and significant pressure dependence, characterized by $\Delta V^{\neq}$. The negative values of $\Delta V^{\neq}$ indicate that all reaction steps are accompanied by extensive solvation related to charge creation in the activation process.[33] The similar value of $\Delta V^{\neq}$ for the two slow comproportionation processes indicates that these reactions proceed with similar changes of charge and solvation effects.

Conclusion

We have spectroscopically observed and kinetically characterized a reactive intermediate $(TCA^{+\bullet})_2$ in the reaction of dibenzoazepine derivatives with cerium(IV). The intermediate subsequently undergoes further degradation, proceeding to another intermediate $(HTCA^+)_2$ and then to the final product. EPR results provide clear evidence for the formation of the intermediate dibenzoazepine $(TCA^{+\bullet})_2$ radical. Neither the further intermediate nor the final product have radical character and showed no signal in EPR. Taking into account the negative values of $\Delta V^{\neq}$ and $\Delta S^{\neq}$ for the electron transfer reaction between cerium(IV) and these organic species it can be concluded that this reaction proceeds *via* an outer-sphere mechanism. The nitrogen atom in the dibenzoazepine moiety does not demonstrate nucleophilic properties. For that reason, the suggested outer-sphere mechanism can also be supported by

Table 5 The activation parameters for the electron-transfer reaction between dibenzoazepine derivatives and the cerium(IV) complexes and the second and third steps of degradation of TCA

Step	TCA	$\Delta H^{\neq}$/kJ mol^{-1}	$\Delta S^{\neq}$/J K^{-1} mol^{-1}	$\Delta V^{\neq a}$/cm^3 mol^{-1}	$\Delta V^{\neq b}$/cm^3 mol^{-1}
I	Imipramine	39 ± 2	−28 ± 8	−10.8 ± 0.2[c]	
	Desipramine	39 ± 2	−28 ± 6		
II	Imipramine	38 ± 2	−13 ± 5	−5.7 ± 0.3	−11.4 ± 0.2
	Desipramine	37 ± 4	−15 ± 12		
III	Imipramine	43 ± 0.3	−7 ± 1	−6.2 ± 0.2	−15.1 ± 0.4
	Desipramine	40 ± 2	−20 ± 8		

[a] [TCA] = 3×10^{-3} M, T = 298 K, [b] [TCA] = 5×10^{-3} M, T = 298 K, [c] [TCA] = 5×10^{-4} M, T = 278 K.

the low ability of dibenzoazepine derivatives to coordinate with transition metal ions.

Acknowledgements

This research was supported by the Nicolaus Copernicus University under grant 379-Ch. The authors would like to thank Dr Erika Ember for her help in the CV measurements.

References

1 F. Kiani, A. A. Rostami, F. Gharib, S. Sharifi and A. Bahadory, *J. Chem. Eng. Data*, 2011, **56**, 2830.
2 A. Simon, C. Ballai, G. Lente and I. Fábián, *New J. Chem.*, 2011, **35**, 235.
3 J. Diwu, S. Wang, Z. Liao, P. C. Burns and T. E. Albrecht-Schmitt, *Inorg. Chem.*, 2010, **49**, 10074.
4 V. Sridharan and J. C. Menéndez, *Chem. Rev.*, 2010, **110**, 3805.
5 R.-S. Hou, H.-M. Wang, I.-J. Kang, H.-D. Du and L.-C. Chen, *Heterocycles*, 2010, **81**, 689.
6 S.-F. Li, X.-M. Zhang, Z.-J. Yao, R. Yu, F. Huang and X.-W. Wei, *J. Phys. Chem. C*, 2009, **113**, 15586.
7 V. Sridharan, P. Ribelles, M. T. Ramos and J. C. Menéndez, *J. Org. Chem.*, 2009, **74**, 5715.
8 G. Lente, J. Kalmár, Z. Baranyai, A. Kun, I. Kék, D. Bajusz, M. Takács, L. Veres and I. Fábián, *Inorg. Chem.*, 2009, **48**, 1763.
9 S. V. More, M. N. V. Sastry and Ch.-F. Yao, *Green Chem.*, 2006, **8**, 91.
10 H. B. Kagan, *Chem. Rev.*, 2002, **102**, 1805.
11 J. B. Moffat, in *Chemistry, Energy and Environment*, ed. C. A. C. Sequeira and J. B. Moffat, The Royal Society of Chemistry, Cambridge, 1998, p. 167.
12 N. N. Greenwood and A. Earnshaw, *Chemistry of the Elements*, 2nd edn, Butterworth-Heinemann, Amsterdam, 2008, 1233.
13 A. M. M. Doherty, M. D. Radcliffe and G. Stedman, *J. Chem. Soc., Dalton Trans.*, 1999, 3311.
14 L. Helm and A. E. Merbach, *Chem. Rev.*, 2005, **105**, 1923.
15 S. B. Hanna, R. R. Kessler, A. Merbach and S. Ruzicka, *J. Chem. Educ.*, 1976, **53**, 524, and references therein.
16 K. G. Everett and D. A. Skoog, *Anal. Chem.*, 1971, **43**, 1541.
17 N. Sussmanand and S. Stahl, *Am. J. Med.*, 1996, **101**, 26S.
18 M. Bourin and G. G. Baker, *Biomed. Pharmacother.*, 1996, **50**, 7.
19 S. N. Frank, A. J. Bard and A. Ledwith, *J. Electrochem. Soc.*, 1975, **122**, 898.
20 T. A. Ivandini, B. V. Sarada, C. Terashima, T. N. Rao, D. A. Tryk, H. Ishiguro, Y. Kubota and A. Fujishima, *J. Electroanal. Chem.*, 2002, **521**, 117.
21 E. Bishop and W. Hussein, *Analyst*, 1984, **109**, 73.
22 (*a*) R. van Eldik, D. A. Palmer, R. Schmidt and H. Kelm, *Inorg. Chim. Acta*, 1981, **50**, 131; (*b*) R. van Eldik, W. Gaede, S. Wieland, J. Kraft, M. Spitzer and D. A. Palmer, *Rev. Sci. Instrum.*, 1993, **64**, 1355.
23 J. Bassett, R. C. Denney, G. H. Jeffery and J. Mendham, *Vogel's Textbook of Qualitative Inorganic Analyses*, Longman, London, 1981, p. 364.
24 A. Mills and A. Cook, *J. Chem. Soc., Faraday Trans. 1*, 1988, **84**, 1691.
25 L. T. Bugaenko and H. Kuan-lin, *Russ. J. Inorg. Chem.*, 1963, **8**, 1299.
26 H. L. Greenhaus, A. M. Feibush and L. Gordon, *Anal. Chem.*, 1957, **29**, 1531.
27 R. H. Abu-Eittah, S. A. Marie and M. B. Salem, *Can. J. Anal. Sci. Spectrosc.*, 2004, **49**, 248.
28 A. M. Horria, *Anal. Lett.*, 1992, **25**, 63.
29 R. G. Wilkins, *Kinetics and Mechanism of Reactions of Transition Metal Complexes*, 2nd edn, VCH, Weinheim, 1991, p. 18.
30 T. A. Ivandini, B. V. Sarada, C. Terashima, T. N. Rao, D. A. Tryk, H. Ishiguro, Y. Kubota and A. Fujishima, *J. Electroanal. Chem.*, 2002, **521**, 117.
31 R. A. de Toledo, M. C. Santos, K. M. Honório, A. B. F. da Silva, E. T. G. Cavalheiro and L. H. Mazo, *Anal. Lett.*, 2006, **39**, 507.
32 M. Neptune, R. L. McCreery and A. Mania, *J. Med. Chem.*, 1979, **22**, 196.
33 (*a*) C. D. Hubbard and R. van Eldik, in *Physical Inorganic Chemistry. Principles, Methods and Models*, ed. A. Bakac, Wiley, New York, 2010, p. 269; (*b*) C. D. Hubbard and R. van Eldik, *Inorg. Chim. Acta*, 2010, **363**, 2357 (Special Issue dedicated to Fred Basolo).